NASA TECHNICAL NOTE

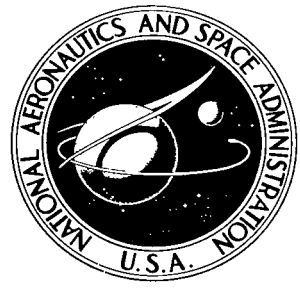

NASA TN D-5741

NASA TN D-5741

A STUDY OF THE ACCURACY OF A FLIGHT-HEATING SIMULATION AND ITS EFFECT ON LOAD MEASUREMENT

by Roger A. Fields

Flight Research Center
Edwards, Calif.

NATIONAL AERONAUTICS AND SPACE ADMINISTRATION • WASHINGTON, D. C. • APRIL 1970

1. Report No.	2. Government Accession No.	3. Recipient's Catalog No.
NASA TN D-5741		

4. Title and Subtitle	5. Report Date
A STUDY OF THE ACCURACY OF A FLIGHT-HEATING SIMULATION AND ITS EFFECT ON LOAD MEASUREMENT	April 1970
	6. Performing Organization Code
7. Author(s)	8. Performing Organization Report No.
Roger A. Fields	H-597
9. Performing Organization Name and Address	10. Work Unit No.
NASA Flight Research Center P. O. Box 273 Edwards, California 93523	126-14-01-01-24
	11. Contract or Grant No.
	13. Type of Report and Period Covered
12. Sponsoring Agency Name and Address	Technical Note
National Aeronautics and Space Administration Washington, D. C. 20546	14. Sponsoring Agency Code

15. Supplementary Notes

16. Abstract

A series of laboratory heating tests simulating the flight heating on an X-15 horizontal stabilizer was conducted. The initial test simulated, as nearly as reasonably possible, the temperatures that were recorded during an X-15 flight to a Mach number of 4.63. Ten additional heating tests were conducted during which inaccuracies were introduced into the flight-heating simulation. The objective of these tests was to establish the effect of the inaccuracies on the strain-gage responses and ensuing load measurements. Strain-gage-bridge responses from all tests were reviewed and compared with those calculated for a stabilizer load of 6000 pounds force (26,700 newtons). The tests were shown to be useful for selecting bridges for use in load-equation derivations and for selecting the equations that yield load measurements with the lowest overall error.

17. Key Words Suggested by Author(s)	18. Distribution Statement
Flight-heating simulation - Flight-load measurement	Unclassified - Unlimited

19. Security Classif. (of this report)	20. Security Classif. (of this page)	21. No. of Pages	22. Price *
Unclassified	Unclassified	27	$3.00

*For sale by the Clearinghouse for Federal Scientific and Technical Information, Springfield, Virginia 22151.

A STUDY OF THE ACCURACY OF A FLIGHT-HEATING SIMULATION AND ITS EFFECT ON LOAD MEASUREMENT

Roger A. Fields
Flight Research Center

SUMMARY

A series of laboratory heating tests simulating the flight heating on an X-15 horizontal stabilizer was conducted. The initial test simulated, as nearly as reasonably possible, the temperatures that were recorded during an X-15 flight to a Mach number of 4.63. Ten additional heating tests were conducted during which inaccuracies were introduced into the flight-heating simulation. The objective of these tests was to establish the effect of the inaccuracies on the strain-gage responses and ensuing load measurements. Responses from the latter 10 simulations were compared with those from the initial test; responses from all simulation tests were compared with those calculated for a stabilizer load of 6000 pounds force (26,700 newtons).

Equations for determining loads (shear, bending, and torque) were developed; the results of the simulation tests were used as a basis for selecting the strain-gage bridges to be included in each equation. Standard-deviation calculations were performed on the equations and the data from the simulations. The simulation tests were shown to be a valuable tool for determining the equations that yield load measurements with the lowest overall error.

Loads were calculated from the equations that would be indicative of load errors to be expected if the strain-gage outputs due to thermal effects were neglected. These loads were so large and unpredictable that, if ignored, they would render flight-loads measurements useless. Heating simulation was shown to be an effective method for isolating the temperature effects of strain-gage measurements, thus permitting the use of strain gages to measure aerodynamic loads in a severe thermal environment.

INTRODUCTION

The measurement of flight loads on aircraft lifting surfaces and control surfaces, particularly on research, developmental, and prototype vehicles, is commonly a vital requirement. Such loads are ordinarily determined by means of either pressure measurements or strain measurements. This report deals only with the determination of flight loads from strain measurements.

If there are no significant thermal effects, the procedure for using strain measurements to obtain flight loads is well established and documented in reference 1. However, when flight speeds increase until there are substantial changes in the temperature

of the load-carrying structure, the strain-gage responses include thermal effects as well as effects due to aerodynamic loads. The load-measurement problem then becomes much more difficult. If the thermal strains are overlooked or disregarded, the load measurements may be so much in error as to be useless. Thus, the problem is to find a way to eliminate the part of the strain-gage response that is due to thermal effects.

One approach to the problem is to fly an aircraft to obtain in-flight strain-gage data which include responses due to both aerodynamic loads and thermal effects. At the same time or during an identical flight, enough temperature data are taken to establish the temperature distribution of the entire structure of interest as a function of time. The flight vehicle, or at least the component for which load measurements are desired, is then reheated on the ground in a manner which duplicates the temperature history of the flight. Thus, the same thermal effects are present on the ground as during flight, but there are no aerodynamic loads. The difference between the strains measured in flight and those measured on the ground represents the strains due to aerodynamic load. The residual strains obtained in this way are then used to obtain loads in the same manner as described in reference 1.

If the temperature simulation on the ground duplicates the flight history perfectly at every point throughout the structure, and if all flight and ground measurements are totally accurate, the method should give good results. As a practical matter, neither perfect temperature simulation nor measurements without error are possible. Thus, before this method for determining flight loads can be used with confidence, the accuracy of the temperature simulation that is reasonably possible must be compared with the accuracy that is necessary to obtain acceptable loads measurements.

Ground tests designed to study the accuracy of tests to simulate flight heating and the consequential effect upon loads measurement were made at the NASA Flight Research Center. Temperatures, but not strains, were measured on the horizontal stabilizer of an X-15 airplane during a high-temperature flight. The stabilizer was then tested on the ground to see how well the temperature distribution could be reproduced, and the results were reported in reference 2. Finally, a series of tests was conducted in which known surface-temperature errors were introduced in order to observe the effect on the strain-gage responses. The results of these tests are presented and discussed in this report in an effort to resolve questions concerning the required accuracy of simulation.

SYMBOLS

The units used for physical quantities in this report are given in U. S. Customary Units and the International System of Units (SI). Factors relating the two systems are presented in reference 3; those used herein are given in the appendix.

A_k kth coefficient of shear equation, pounds/μ (newtons/μ)

B_k kth coefficient of bending-moment equation, foot-pounds/μ (meter-newtons/μ)

$\bar{C}_k$	kth coefficient of torque equation, foot-pounds/μ (meter-newtons/μ)
m	number of coefficients in load equation
δ	strain-gage-bridge output
δ_{cal}	strain-gage-bridge output due to shunt-calibration resistor
δ_o	data reference (zero) for strain-gage bridges
μ	nondimensional strain-gage-bridge output
σ	standard deviation

Subscripts:

b	bending-moment equation
g	strain-gage-bridge output
k	load-equation-term index (k = 1, 2, 3 .... m)
s	shear equation
t	torque equation

TEST SETUP

Test Article

The X-15 horizontal stabilizer used for the tests on which this report is based represented a structure particularly sensitive to the problems of high-temperature loads measurements. The X-15 is a single-place, rocket-powered airplane (see ref. 4 for additional specifications) that was carried aloft by a B-52 aircraft and launched at a Mach number of 0.82 and an altitude of 46,700 feet (14,230 meters) for the flight discussed in this report. On this flight a maximum Mach number of 4.63 and a maximum altitude of 84,400 feet (25,730 meters) were obtained. Because of the high speed, the horizontal stabilizer developed both high temperatures and high heating rates (up to 15° F/sec or 8.3° K/sec). The stabilizer temperature data recorded during the flight were used for the simulation tests of this report.

The stabilizer was an all-movable surface located far aft on the airplane, as shown in figure 1. It served for both pitch and roll control and consisted of a stiff structure made of three materials having dissimilar coefficients of thermal expansion. Except for abrupt maneuvers, the aerodynamic loads were usually quite small; consequently, the normal condition was one of high thermal strain and low strain due to aerodynamic loads. Also, the stabilizer was a small structure with only one primary load-carrying member, which limited the number of practical strain-gage locations and required utilization of gages that had less than optimum performance. Thus, the X-15 horizontal stabilizer represented a load-measuring problem more severe than that of similar control surfaces on most aircraft.

E-7910

Figure 1. X-15 aircraft.

Basic dimensions and structural details of the stabilizer are shown in figure 2. The total exposed surface area was approximately 52 square feet (4.8 square meters). Additional structural details are presented in reference 2.

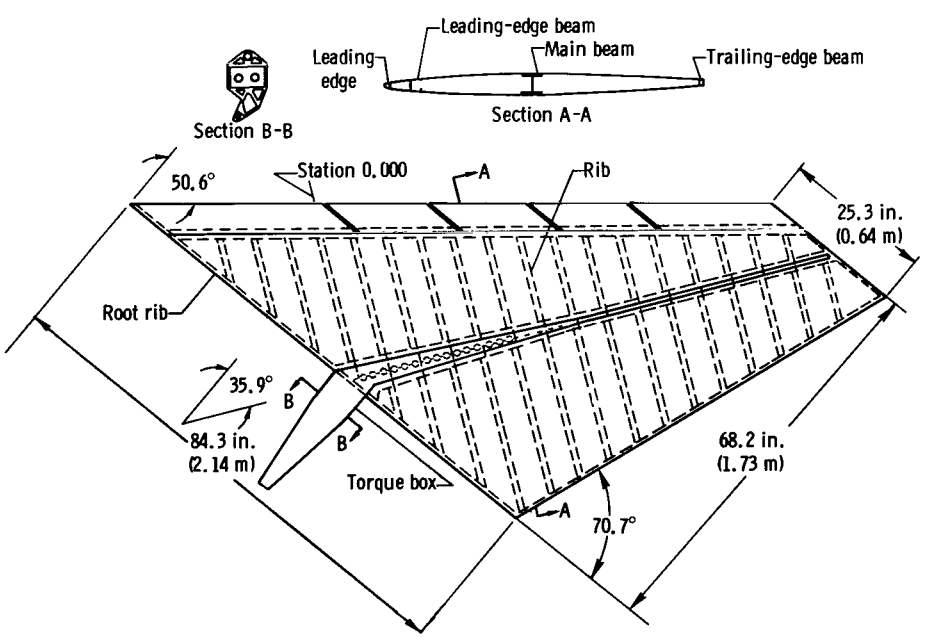

Figure 2. X-15 horizontal-stabilizer structure.

Strain-Gage Instrumentation

The stabilizer was instrumented internally with strain gages when it was being constructed, and several additional strain gages were installed on the outside surface of the torque box (fig. 2) after the construction was completed. The locations, types, and numbers of the strain-gage bridges used in the subject tests are shown in figure 3.

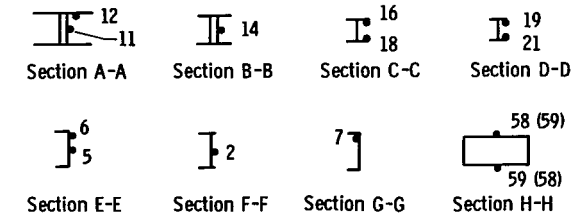

Strain-gage bridges

Type	Number
Shear	2, 5, 11, 14
Bending	6, 7, 12, 16, 18, 19, 21
Torque	58, 59

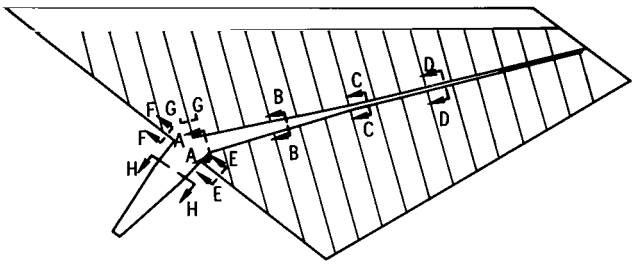

Figure 3. Locations, types, and numbers of strain-gage bridges.

Table I lists the strain-gage-bridge numbers and the corresponding types of strain gages and primary specifications. The gage factors for all the types of strain gages listed were specified to vary inversely with temperature at a rate of 1 percent per

TABLE I. – STRAIN-GAGE SPECIFICATIONS

Strain-gage-bridge numbers	Model number	Manufacturer	Type	Nominal gage resistance (per element), ohms	Operable temperature range (static strain measurements), °F (°K)	Nominal gage factor
11, 14	SG 101	Microdot Inc.	Single-element weldable	120	-320 to 650 (78 to 617)	1.55
58, 59	SG 321	Microdot Inc.	Half-bridge weldable	120	-452 to 650 (4 to 617)	1.75
2, 5, 6, 7, 12, 16, 18, 19, 21	SG 420	Microdot Inc.	Half-bridge weldable	115	-452 to 950 (4 to 783)	3.5*

*Compensated gage factor.

100° F (56° K) throughout the compensated temperature range.

Figure 4 shows typical apparent strain[1] curves for all the bridge configurations and types of strain gages used. The apparent strain, normally presented in micro-strain, was nondimensionalized by using a 250,000-ohm shunt-calibration resistor; this makes the apparent strain data more directly comparable with data presented later in this report. The strain gages were mounted on coupons of Inconel-X.

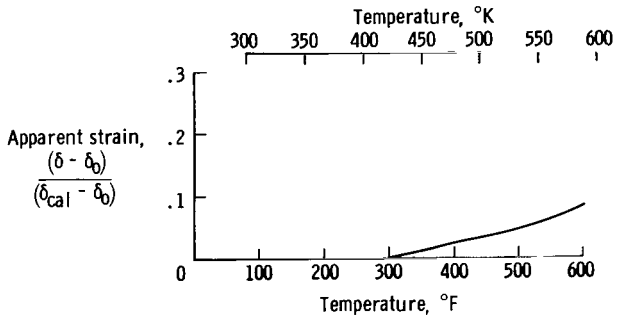

(a) Strain-gage model SG 101; shear bridge; 8.5° F/sec (4.7° K/sec) heating rate; 5-volt bridge excitation.

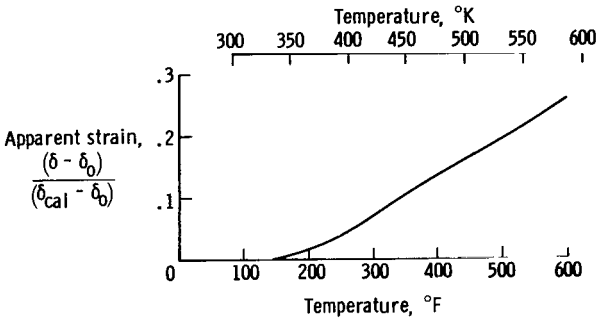

(b) Strain-gage model SG 321; shear bridge; 8.5° F/sec (4.7° K/sec) heating rate; 5-volt bridge excitation.

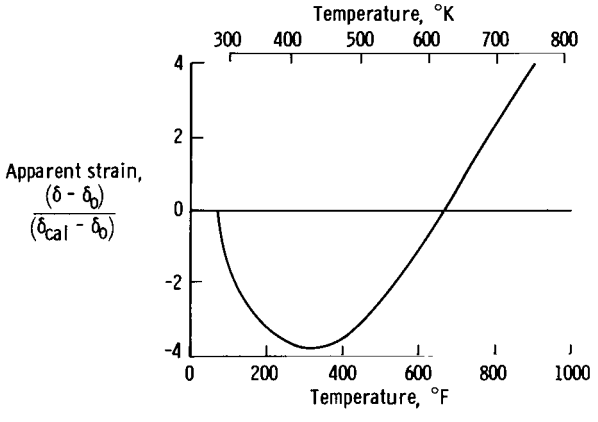

(c) Strain-gage model SG 420; bending bridge; 10° F/sec (5.6° K/sec) heating rate; 6-volt bridge excitation.

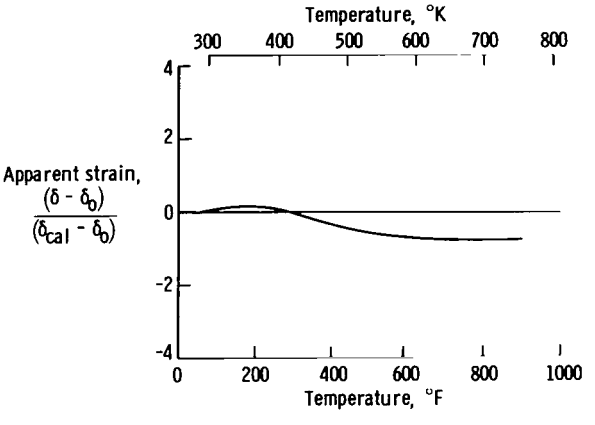

(d) Strain-gage model SG 420; shear bridge; 10° F/sec (5.6° K/sec) heating rate; 5-volt bridge excitation.

Figure 4. Typical apparent-strain curves.

Thermocouples were installed at all strain-gage-bridge locations and their outputs were recorded during the tests. The thermocouple numbers corresponding to bridges 58 and 59 were 158 and 159, respectively; the remaining thermocouples and their corresponding bridges have identical numbers.

[1]The apparent strain indicated by a strain gage or bridge is primarily due to the difference between the coefficients of thermal expansion of the gage and the material upon which it is mounted.

Figure 5 shows examples of the internal instrumentation installation. Figure 5(a) shows half of a bending bridge on the main-beam cap and half of a shear bridge on the corrugated web of the main beam. The remainders of these two bridges are on the opposite side of the beam. These installations are typical of those along the main beam. Figure 5(b) shows two full bending bridges and one shear bridge which are typical of the bridges on the ribs.

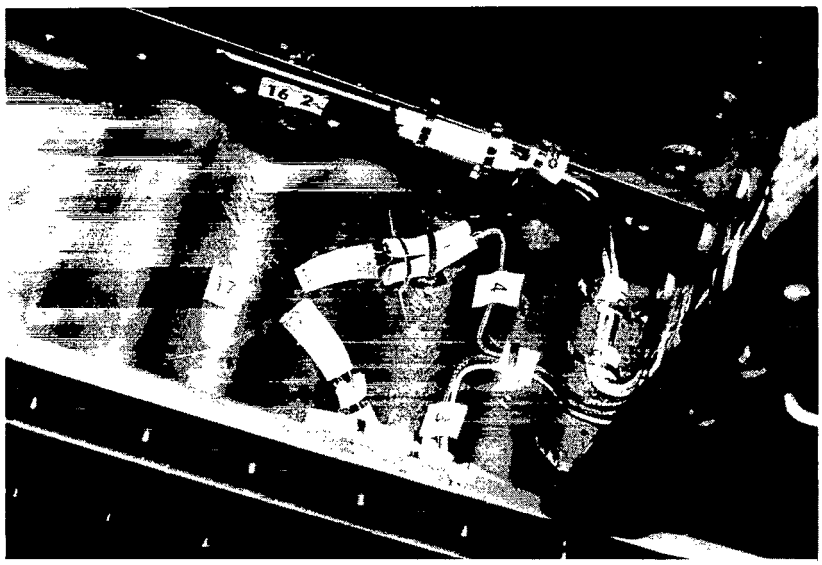

E-16005

(a) Main beam.

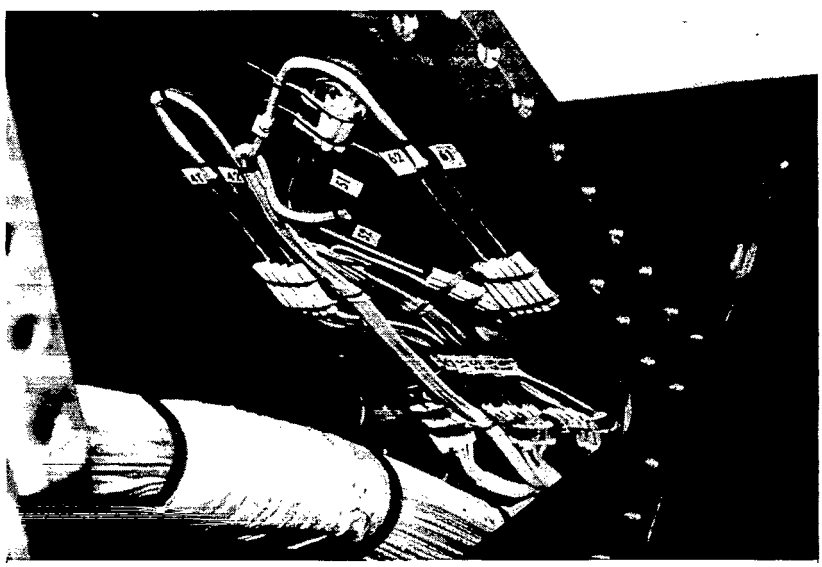

E-16008

(b) Root rib.

Figure 5. Examples of strain-gage installations on the main beam and the root rib.

Data-Acquisition System

The test data were recorded with the data-acquisition system of the High Temperature Loads Calibration Laboratory at the Flight Research Center. The system can record voltages in 5 ranges, varying from ±5.0 millivolts full scale with a resolution of 2.5 microvolts to ±4.0 volts with a resolution of 2.0 millivolts. The strain-gage data were recorded in the most sensitive range at the beginning of the tests and were automatically changed to the next higher range if necessary during a test. The signals were commutated at a rate of 10 samples per second and recorded on magnetic tape. Errors in the data due to the acquisition system were negligible. Additional information about the data-acquisition system is presented in references 2 and 5.

Laboratory Simulation Equipment

The temperature simulation on the horizontal stabilizer required a cool-down and cold-soak for the portion of the flight during which the X-15 was carried to altitude by the B-52 launch aircraft. A system utilizing liquid nitrogen provided the cooling. The liquid nitrogen was sprayed into ambient air in a chamber where it evaporated and mixed with the air, thereby cooling it to the desired temperature. The cooled air was then directed to the stabilizer by a system of ducts.

The simulation of the part of the flight after the X-15 was launched required heating, which was provided by radiant heating from infrared lamps. The lamps were mounted on polished stainless-steel reflectors and distributed in a manner which provided the highest heat flux over major heat sinks. The lamps were divided into zones as shown in figure 6. Zones 1 to 5 provided heating for the leading edge and root rib; the other zones were identical for the two reflectors which heated the upper- and lower-stabilizer surfaces. Each zone consisted of a specific group of lamps and was controlled independently with a closed-loop system. The temperature on the stabilizer, recorded by a thermocouple at a single location in each zone, was maintained by the lamps according to a preprogramed temperature time history. For these tests the temperature time histories were those recorded during the X-15 flight.

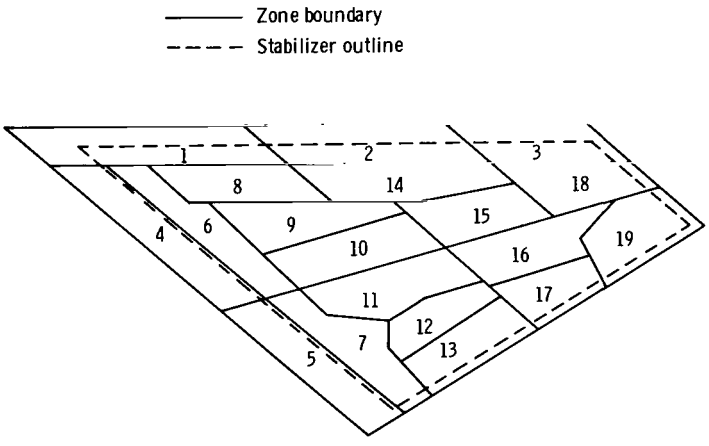

Figure 6. X-15 horizontal-stabilizer heating-simulation zones.

The overall simulation test setup is shown in figure 7, and additional information about the simulation equipment is presented in references 2 and 5.

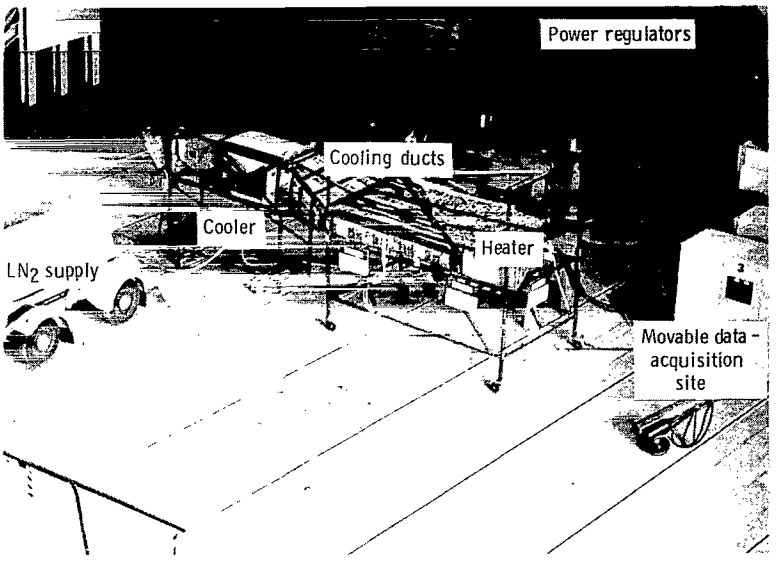

E-19429

Figure 7. Overall heating-simulation test setup.

STRAIN-GAGE CALIBRATION AND EQUATION DERIVATION

During simulation tests and strain-gage calibration, the stabilizer was mounted in a laboratory fixture which duplicated the attachment on the X-15 airplane. Prior to strain-gage calibration, the stabilizer was subjected to a series of heat and load cycles to establish strain-gage repeatability. The calibration was accomplished by applying a series of single-point loads at locations distributed over the stabilizer surface. The calibration load points and the corresponding maximum loads are shown in figure 8. The loading was applied with hydraulic actuators through 8-inch by 18-inch (20.3-centimeter by 45.7-centimeter) compression load pads. The loads were applied and recorded continuously from zero to maximum load and back to zero. Strain-gage-bridge signals were recorded simultaneously with the loads. The data were nondimensionalized to the following expression:

$$\mu = \frac{(\delta - \delta_o)}{(\delta_{cal} - \delta_o)}$$

A least-squares method was used to determine slopes (μ per unit load) for all load points for each bridge. The slopes were then entered into a computer program which calculated coefficients for shear, bending moment, and torque equations by using a series of matrix operations to solve the least-squares normal equation (eq. (14)) of reference 1. After determining the coefficients, the program calculated loads from the equations by using the original input data (slopes). These values were then compared with the actual applied loads and an average absolute error established for each equation.

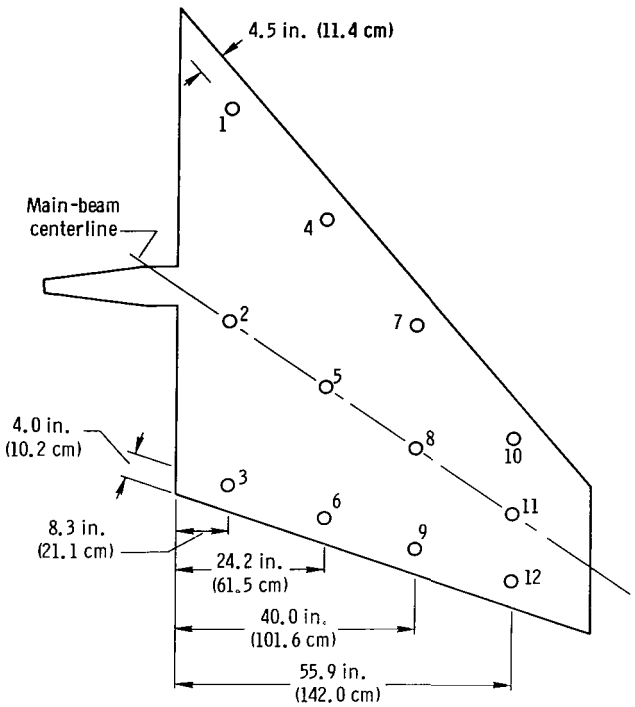

Load point	Maximum load, lbf (N)
1	1400 (6227)
2	1400 (6227)
3	1400 (6227)
4	1400 (6227)
5	1400 (6227)
6	1400 (6227)
7	1400 (6227)
8	1400 (6227)
9	1400 (6227)
10	700 (3114)
11	700 (3114)
12	700 (3114)

Figure 8. Calibration load points and corresponding maximum loads.

The equations thus derived were then used to compute shear, bending moment, and torque from measured strain-gage-bridge outputs. The loads calculated in this way may be due to several factors such as airload, thermal strain, inertia effects, apparent strain, or other miscellaneous temperature-induced effects[1].

TEST PROCEDURE

The heating simulation presented in reference 2 was considered the standard for these tests. The procedure used in the study of reference 2 to simulate the flight temperature time history on the stabilizer was as follows:

1. Cool-down and cold-soak to X-15 pre-launch conditions.

2. Transfer to heating mode.

3. Conduct the heating test from X-15 launch to approximately 200 seconds after launch.

[1]Among the important temperature-induced effects that might influence calculated loads are the variation of strain-gage gage factor, the change of modulus of elasticity in the stabilizer structure, and the existence of electromotive forces (thermocouple effect) in the strain-gage circuits. The reduction of gage factor at elevated temperature which reduces strain-gage-bridge outputs is partly compensated for by the increase in outputs due to the decrease in structural modulus. The decrease in modulus of elasticity (15 percent at 800° F (700° K)) for Inconel-X is approximately linear to 800° F (700° K). The thermocouple effect on strain gages is considered to be small.

The maximum absolute average temperature deviations between the flight-measured temperatures and those simulated during the ground heating tests in step 3 were established to be less than 50 F° (27.8 K°) (ref. 2). With this as a guideline, a series of 10 tests was performed in which intentional variations or errors were introduced into the flight-temperature simulation. The conditions and affected zones for these tests are listed in table II. The purpose of the temperature-variation tests was to provide information on strain-gage-bridge outputs and the resulting load-measurement errors because of inherent inaccuracies in the heating simulation.

TABLE II. – SIMULATION-VARIATION TESTS

Test number	Stabilizer area	Simulation variation	Zones affected
1	Entire stabilizer	No cooling	All
2	Leading edge	Temperature reduction	1, 2, 3
3	Root rib	Temperature reduction	4, 5
4	Main beam (top surface)	Temperature reduction	10, 11, 15, 16, 18
5	Forward of main beam (top surface)	Temperature reduction	1, 2, 3, 6, 8, 9, 10, 14, 15, 18
6	Aft of main beam (top surface)	Temperature reduction	7, 11, 12, 13, 16, 17, 19
7	Outboard half (top surface)	Temperature reduction	2, 3, 14-19
8	Inboard half (top surface)	Temperature reduction	1, 6-13
9	Entire top surface	Temperature reduction	All except 4, 5
10	Entire stabilizer	Temperature reduction	All

The variations were selected to provide temperature errors at the leading edge and main beam, at zones in which the strain-gage bridges were directly heated, and at a variety of surface areas. Most of the variations introduced a temperature error on only one side of the stabilizer. This caused a change in the temperature gradient through the stabilizer, resulting in thermal stresses and strains that were larger than if the error had been introduced on both sides simultaneously.

The first variation consisted of no cool-down or cold-soak; this affected the entire stabilizer and presented a considerable deviation from the flight-measured temperature time history. The purpose of the variation was to determine if it was essential to include the cool-down and cold-soak in the overall simulation.

The last nine variations consisted of reductions in temperatures that were programed for the standard test by a linear function from 0 F° (0 K°) at zero-time (X-15 launch) to 50 F° (27.8 K°) at 135 seconds after launch and a constant 50 F° (27.8 K°) during the remainder of the test. It was assumed that reducing the temperature on one side would produce approximately the same change in the bridge output as increasing the temperature on the opposite side. Therefore, reduced temperatures were programed instead of increased temperatures to prevent overheating the stabilizer or the instrumentation. All zones, except those affected by the variations, were programed for the X-15 flight temperatures. All tests, except the test with no cooling, were conducted in the same manner as the standard test. In each test the heating portion was of primary concern.

RESULTS AND DISCUSSION

Strain-Gage-Bridge Responses

The heating in test 2 (see table II) was only slightly different from that in the standard test. The simulation variation of test 2 was so remote from the strain-gage bridges that the bridge outputs were very similar to those from the standard test. Figure 9 shows the output of bridge 19 for both tests. The difference between the outputs of test 2 and the standard test for this bridge was larger than for any other bridge. The maximum difference was 0.9 (for the nondimensionalized ordinate), which represents 6.4 percent of the total output. This illustrates that the strain-gage responses are essentially repeatable for duplicate or nearly duplicate tests. It also shows that it may not be necessary to duplicate temperatures exactly at areas remote from strain-gage instrumentation.

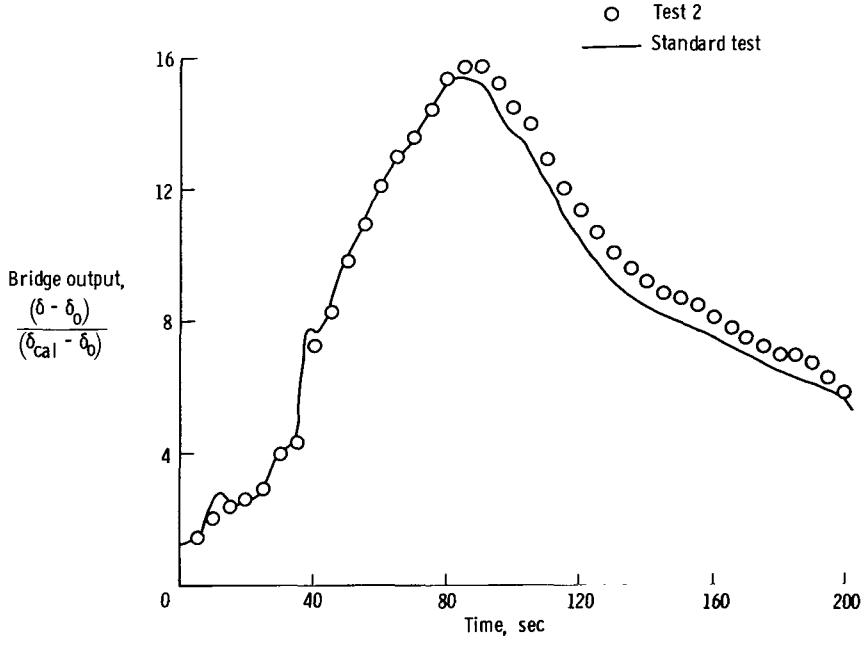

Figure 9. Output of strain-gage bridge 19.

The outputs for each strain-gage bridge for all tests were plotted as functions of time. Figures 10(a) and 10(b) show the bridge outputs for the standard test and a band which includes data from all variation tests except the test with no cooling. However, data from the latter test are shown in the figures by the square symbols; these data were not included in the band because they represent an extreme simulation variation. Most of the no-cooling-test data are outside the band, which points out the need to include cooling in the simulation.

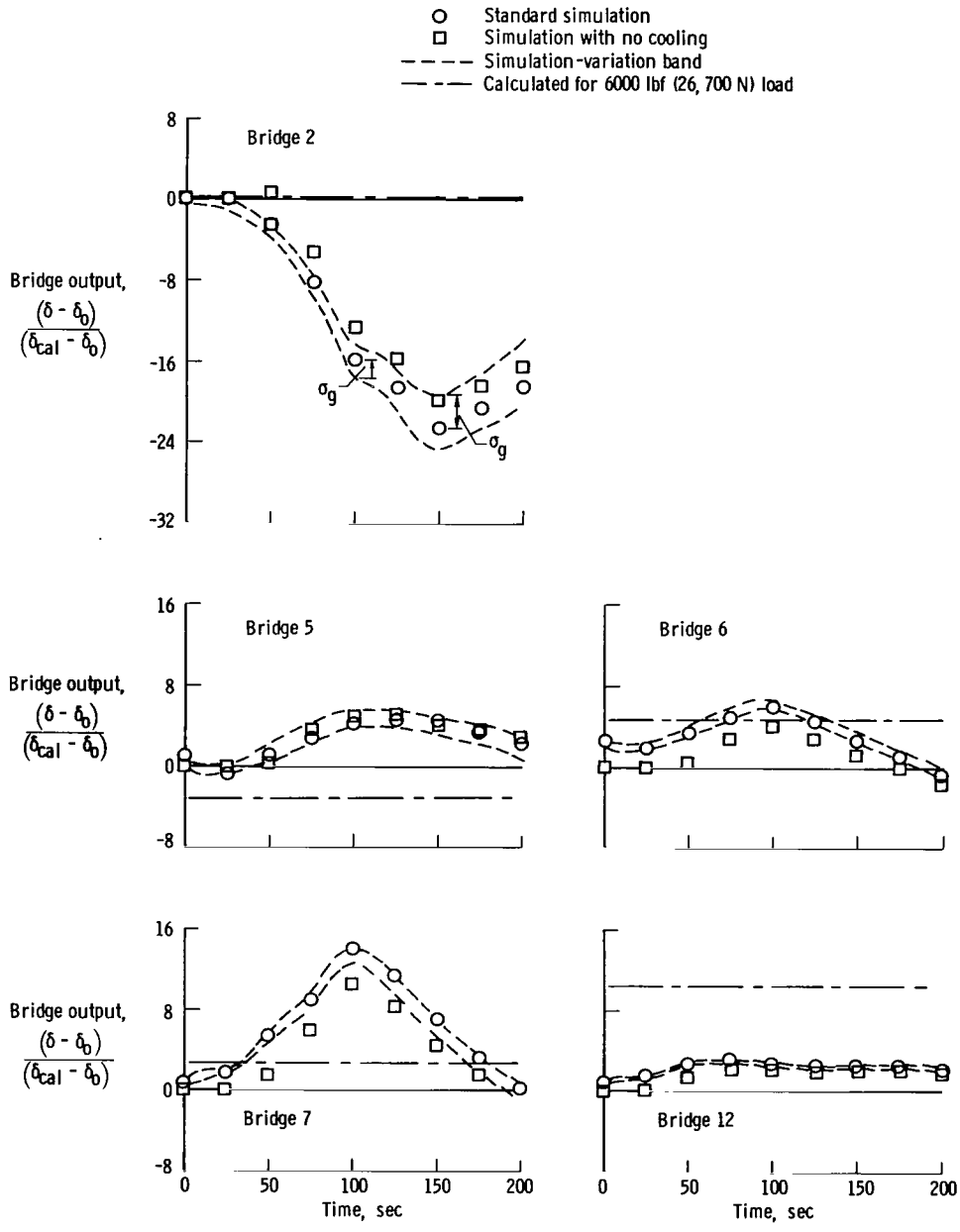

(a) Bridges 2, 5, 6, 7, 12.

Figure 10. Strain-gage-bridge outputs from simulation tests.

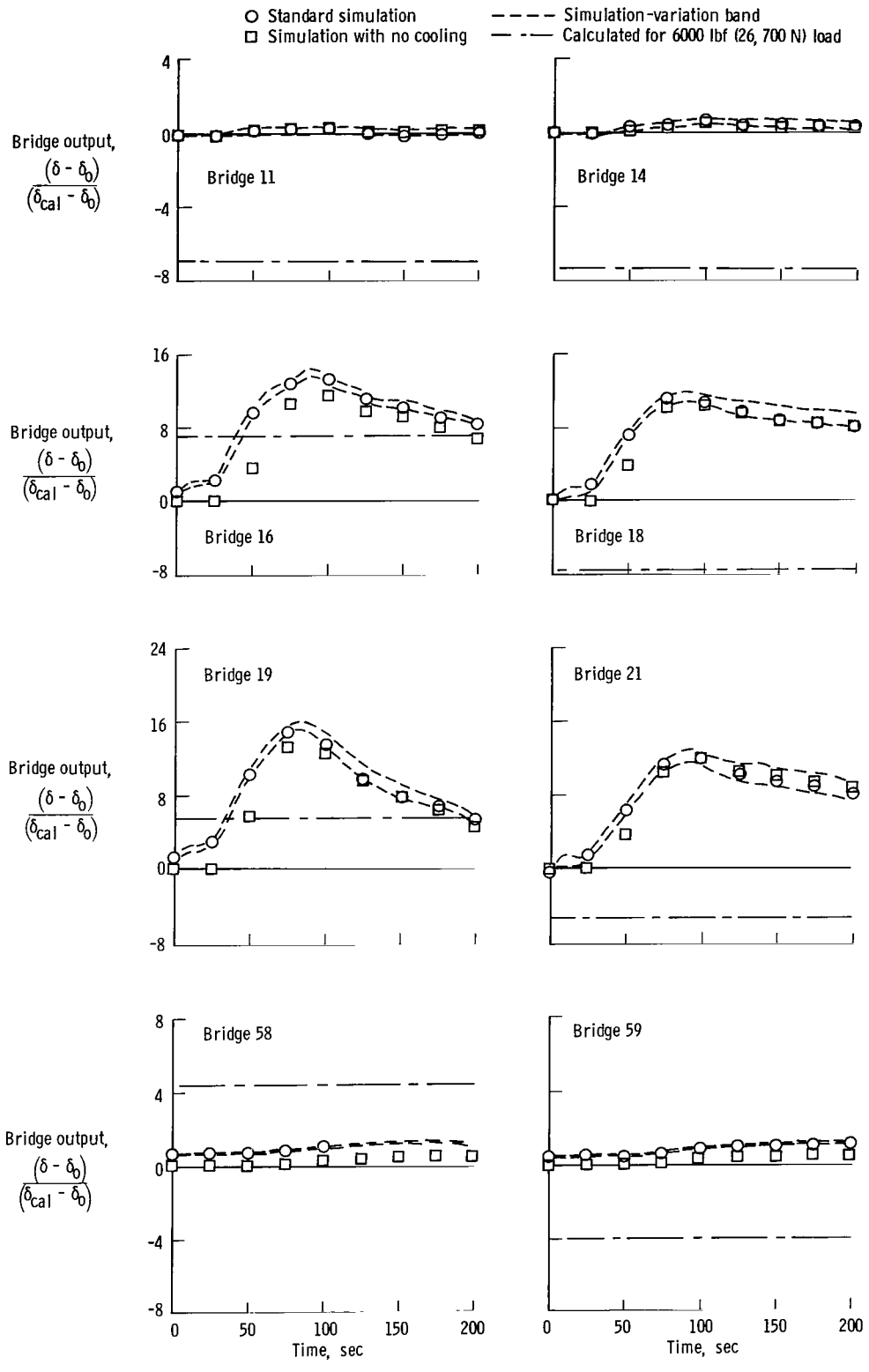

(b) Bridges 11, 14, 16, 18, 19, 21, 58, 59.

Figure 10. Concluded.

All bridges had responses due to the temperature simulation; although a few responses were small, they were still considered significant because of their possible contribution to error in the measured flight loads. Responses were caused primarily by thermal strain and apparent strain. (See fig. 4.) The temperatures at the bridge locations during the standard simulation are shown in figure 11. Most of the strain-gage responses reached their peaks at about 100 seconds after launch, when thermal strain was maximum, because of thermal stresses produced during the high-heating-rate portion of the test. After peak-surface temperatures were reached, the temperature gradients through the stabilizer structure decreased and caused a corresponding decrease in the bridge responses.

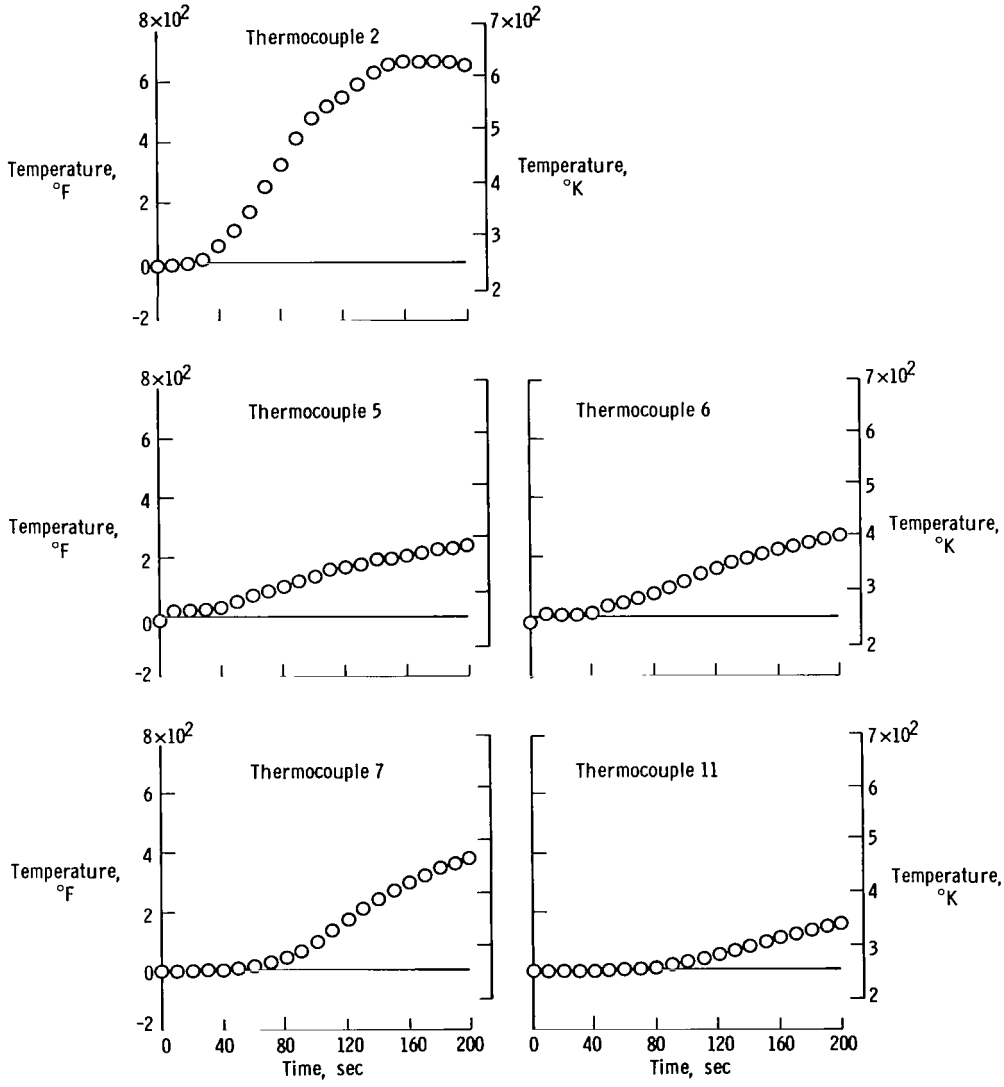

(a) Thermocouples 2, 5, 6, 7, 11.

Figure 11. Temperatures at strain-gage-bridge locations during the standard simulation.

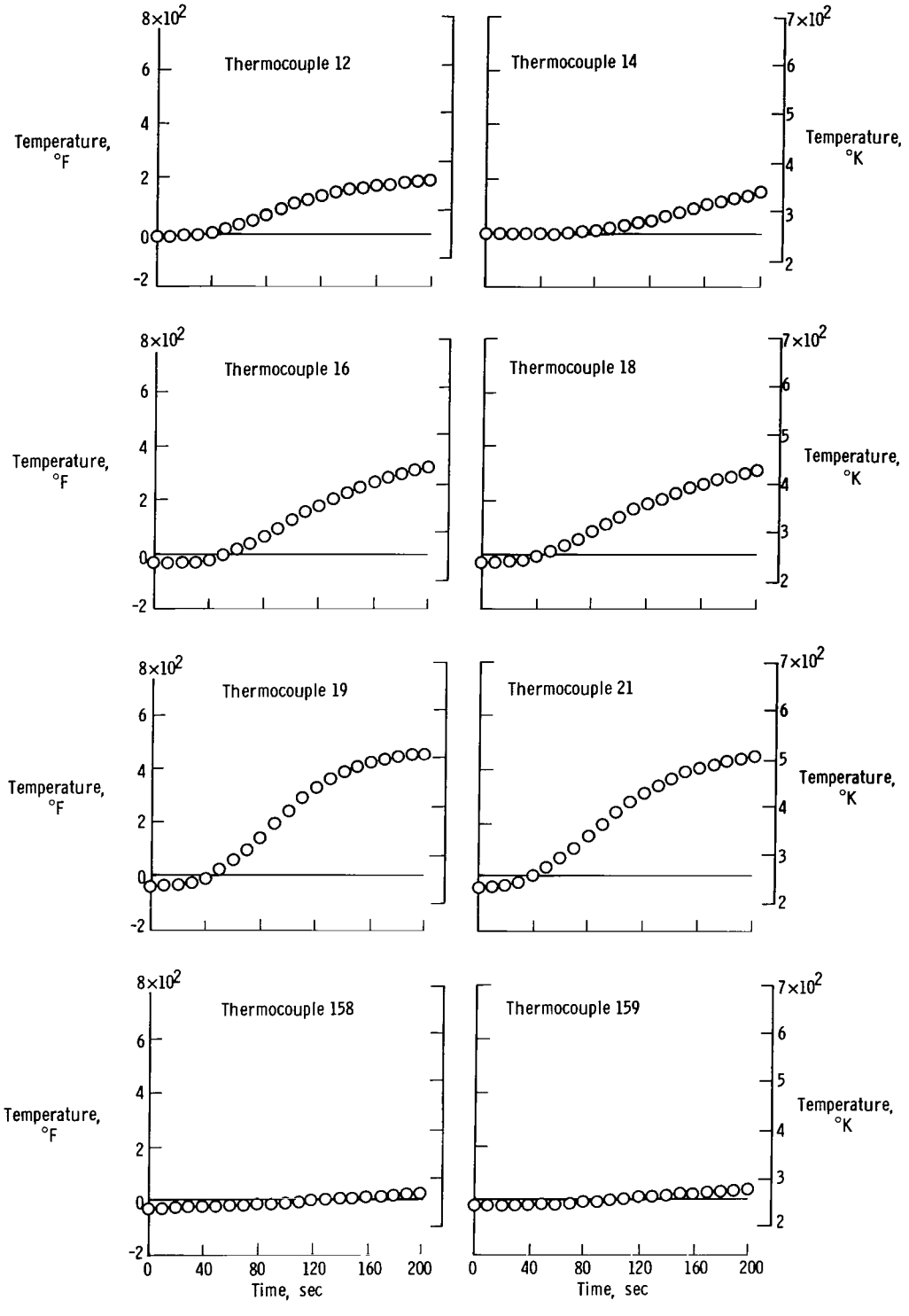

(b) Thermocouples 12, 14, 16, 18, 19, 21, 158, 159.

Figure 11. Concluded.

To provide a comparison between the outputs due to the temperature-simulation tests and outputs that would be produced by an aerodynamic load, bridge outputs were calculated from the calibration data assuming an equally distributed 6000 pounds force (26,700 newtons) load on the surface of the stabilizer. The outputs are plotted as constant lines in figures 10(a) and 10(b). The 6000 pounds force (26,700 newtons) load represents the approximate maximum aerodynamic load that would be introduced on the stabilizer during a typical pull-up/push-over X-15 maneuver. The bending moment and torque due to this load are 16,050 foot-pounds force (21,760 meter-newtons) and -10,850 foot-pounds force (-14,710 meter-newtons), respectively.

The strain-gage data were reviewed with reference to the ratios of (1) output due to simulation temperatures to the calculated-load output and (2) bandwidth to load output. (See fig. 10.) The first ratio indicates the importance of thermal effects and the corresponding need for a simulation test to be performed; the ideal situation of a ratio equal to zero denotes no thermally induced output from a particular bridge. The demand for an accurate simulation increases as the ratio becomes larger because small temperature changes tend to produce larger deviations in the bridge outputs with respect to the load output. The second ratio indicates the significance of simulation inaccuracy; as the ratio increases, the value of performing a simulation to obtain load measurements decreases.

Strain-gage bridges 11, 12, 14, 58, and 59 proved to be the best of those considered in terms of the two ratios; their ratios of simulation output to load output and bandwidth to load output were both small. Bridge 2 exhibited the highest values of both ratios; it was, therefore, excluded from further consideration. The remainder of the bridges had ratios between the two extremes.

Development of Load Equations

A series of load equations for shear, bending moment, and torque was developed by using various combinations of the strain-gage bridges. All the bridges were used in the equations except bridge 2. Table III lists the average absolute error for each equation, the bridge number to which each coefficient applies, and the equation coefficients. The equation-derivation program was written to handle a maximum of six gages per equation; therefore, all equations derived consisted of six gages or less.

When selecting the bridge combinations for the equations, it was necessary to examine the calibration slopes to determine if any of the outputs were redundant, i.e., linear multiples of each other. If there had been a redundancy, a singular matrix would have been formed and no solution would have been possible. If there had been similar outputs, a solution may have been available, but it could have been considerably inaccurate because of the ill-conditioned matrix. The outputs of bridges 58 and 59 were similar except for sign; therefore, these bridges were not used together in an equation. Judging by the relative size of the torque-equation coefficients (equations T9 to T15, table III(c)), these same bridges were nearly self-reliant for determining torque.

To obtain shear equations with low average absolute errors, it seemed to be necessary to include one or more of bridges 5, 6, and 7 in the equations. Bridge 6 was the best of the three in terms of the ratios of simulation output to load output and

TABLE III. – X-15 HORIZONTAL-STABILIZER LOAD EQUATIONS

Equation number	Average absolute error, percent	Bridge number/equation coefficient					
(a) Shear-equation coefficient, lbf/μ (N/μ)							
S1	12.5	7/-188 (-836)	11/-1006 (-4475)	12/-396 (-1761)	14/-241 (-1072)	16/20 (89)	18/-199 (-885)
S2	17.8	11/-699 (-3109)	12/-226 (-1005)	14/-326 (-1450)	16/-301 (-1339)	18/399 (1775)	
S3	18.0	11/-645 (-2869)	14/-225 (-1001)	16/-678 (-3016)	18/-598 (-2660)		
S4	18.0	11/-646 (-2873)	14/-226 (-1005)	16/-638 (-2838)	18/-548 (-2438)	21/-15 (-67)	
S5	7.5	5/1049 (4666)	6/1442 (6414)	11/-1187 (-5280)	12/-773 (-3438)	14/-106 (-471)	16/147 (654)
S6	7.6	6/377 (1677)	11/-979 (-4355)	12/-195 (-867)	14/914 (4065)		
S7	7.3	6/382 (1699)	11/-1040 (-4626)	12/-462 (-2055)	14/-38 (-169)	16/189 (841)	
S8	7.8	6/396 (1761)	11/-1059 (-4710)	12/-502 (-2233)	14/-1 (-4)	16/820 (3647)	18/542 (2411)
S9	16.2	11/-793 (-3527)	12/-144 (-641)	14/-105 (-467)	58/216 (961)		
S10	17.7	11/-740 (-3292)	12/-100 (-445)	14/-145 (-645)	59/-143 (-636)		
S11	4.8	6/642 (2856)	11/-841 (-3741)	12/20 (89)	14/96 (427)	59/606 (2695)	
S12	4.3	6/632 (2811)	11/-872 (-3879)	12/-98 (-436)	14/45 (200)	16/74 (329)	59/578 (2571)
S13	3.6	6/705 (3136)	11/-759 (-3376)	12/68 (302)	58/-746 (-3318)		
S14	3.0	6/743 (3305)	11/-822 (-3656)	12/57 (254)	14/75 (334)	58/-737 (-3278)	
S15	3.0	6/748 (3327)	11/-815 (-3625)	12/83 (369)	14/85 (378)	16/-16 (-71)	58/-747 (-3323)
(b) Bending-moment-equation coefficient, ft-lbf/μ (m-N/μ)							
B1	4.9	7/516 (700)	11/-51 (-69)	12/1543 (2092)	14/488 (662)	16/-617 (-837)	18/-451 (-612)
B2	17.5	11/-895 (-1214)	12/1076 (1459)	14/281 (381)	16/267 (362)	18/1013 (1374)	
B3	18.9	11/-1149 (-1558)	14/-198 (-268)	16/2062 (2796)	18/1048 (1421)		
B4	17.3	11/-1147 (-1555)	14/-194 (-263)	16/1639 (2222)	18/524 (711)	21/161 (218)	
B5	2.7	5/882 (1196)	6/317 (430)	11/-511 (-693)	12/1140 (1546)	14/-183 (-248)	16/76 (103)
B6	6.8	6/-577 (-782)	11/-351 (-476)	12/1559 (2114)	14/-499 (-677)		
B7	6.3	6/-574 (-778)	11/-388 (-526)	12/1402 (1901)	14/-127 (-172)	16/111 (151)	
B8	4.6	6/-609 (-826)	11/-341 (-462)	12/1500 (2034)	14/-218 (-296)	16/-1456 (-1974)	18/-1345 (-1824)
B9	7.1	11/-273 (-370)	12/1806 (2449)	14/28 (38)	58/-897 (-1216)		
B10	9.1	11/-343 (-465)	12/1758 (2384)	14/114 (155)	59/836 (1134)		
B11	4.0	6/-431 (-584)	11/-275 (-373)	12/1678 (2275)	14/-48 (-65)	59/334 (453)	
B12	3.9	6/-438 (-594)	11/-295 (-400)	12/1602 (2172)	14/-81 (-110)	16/49 (66)	59/316 (428)
B13	4.2	6/-330 (-447)	11/-310 (-420)	12/1699 (2304)	58/-426 (-578)		
B14	3.3	6/-361 (-490)	11/-259 (-351)	12/1708 (2316)	14/-60 (-81)	58/-434 (-589)	
B15	3.3	6/-359 (-487)	11/-255 (-346)	12/1722 (2335)	14/-54 (-73)	16/-9 (-12)	58/-440 (-597)
(c) Torque-equation coefficient, ft-lbf/μ (m-N/μ)							
T1	3.1	7/1411 (1913)	11/287 (389)	12/-1408 (-1909)	14/-5 (-7)	16/933 (1265)	18/673 (913)
T2	58.1	11/-2020 (-2739)	12/-2684 (-3640)	14/629 (853)	16/3347 (4539)	18/2183 (2960)	
T3	63.1	11/-1386 (-1879)	14/1822 (2471)	16/-1131 (-1534)	18/-180 (-244)		
T4	61.9	11/-1389 (-1883)	14/1817 (2464)	16/-626 (-849)	18/446 (605)	21/-192 (-260)	
T5	13.9	5/419 (568)	6/290 (393)	11/-1401 (-1900)	12/-3052 (-4139)	14/-688 (-933)	16/553 (750)
T6	23.2	6/-1354 (-1836)	11/-581 (-788)	12/-794 (-1077)	14/77 (104)		
T7	23.0	6/-1337 (-1813)	11/-815 (-1105)	12/-1811 (-2456)	14/-418 (-567)	16/720 (976)	
T8	21.9	6/-1364 (-1850)	11/-778 (-1055)	12/-1733 (-2350)	14/-490 (-664)	16/-522 (-708)	18/-1066 (-1445)
T9	1.3	11/-9 (-12)	12/133 (180)	14/20 (27)	58/-2713 (-3679)		
T10	10.1	11/-152 (-206)	12/51 (69)	14/245 (332)	59/2642 (3583)		
T11	7.0	6/-407 (-552)	11/-88 (-119)	12/-25 (-34)	14/92 (125)	59/2167 (2938)	
T12	8.0	6/-451 (-612)	11/-217 (-294)	12/-511 (-693)	14/-125 (-170)	16/315 (427)	59/2049 (2778)
T13	1.3	6/-27 (-37)	11/5 (7)	12/130 (176)	58/-2689 (-3646)		
T14	1.3	6/-19 (-26)	11/-8 (-11)	12/128 (174)	14/15 (20)	58/-2688 (-3645)	
T15	1.4	6/-13 (-18)	11/1 (1)	12/160 (217)	14/28 (38)	16/-19 (-26)	58/-2701 (-3663)

bandwidth to load output; hence, it was selected for most of the equations. Bridges 16, 18, 19, and 21 were omitted from most of the equations in an effort to use the best bridges and keep the load error due to simulation inaccuracy at a minimum. If equations must be developed using bridges with outputs such as those of bridges 5, 6, 7, 16, 18, 19, and 21, it appears that the number of bridges in the equations should be kept to a minimum, thereby, the load error will usually be minimized. This may be true in other cases when the thermal environment is not a problem, but it is especially necessary when extreme temperatures are present that produce added sources of error in the bridge outputs.

Load-Measurement Accuracy

As an example of the errors in load measurement that would be introduced if a test to simulate flight heating were not performed to correct the data, the strain-gage outputs obtained from the standard simulation were used as inputs [1] to equations S9, S13, S14, B9, B13, B14, T9, T13, and T14; the resulting loads are shown in figure 12.

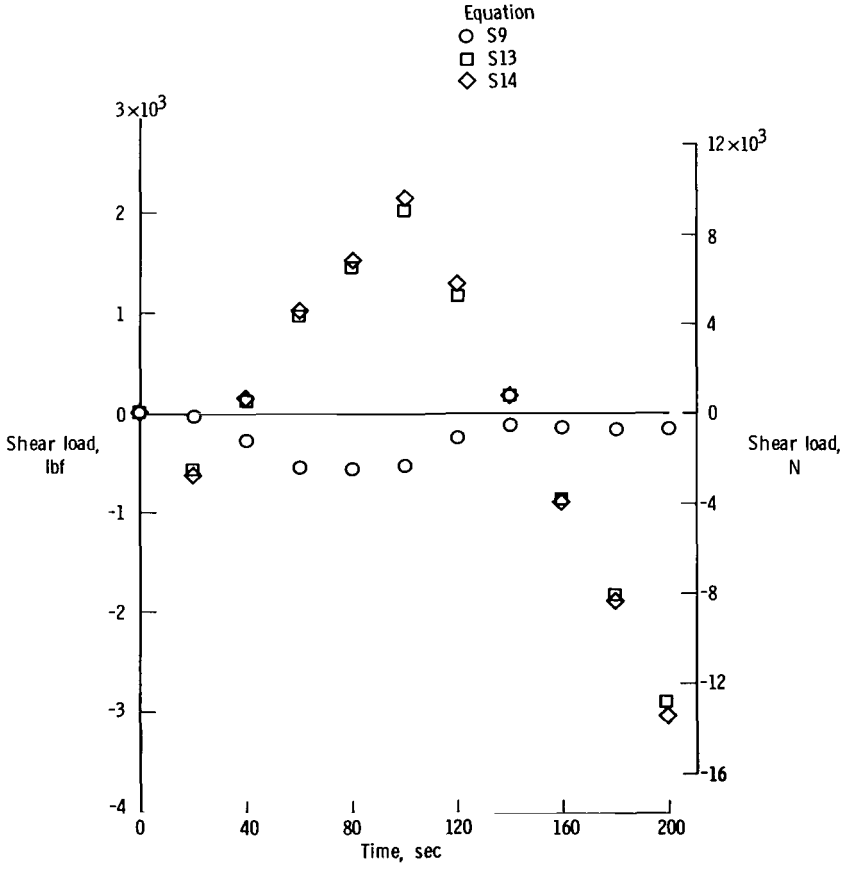

(a) Shear.

Figure 12. Loads resulting from simulation strain-gage-bridge outputs.

[1] No data were obtained from 100 seconds to 200 seconds after launch during the standard simulation with strain-gage bridge 58. An assumed curve (within the band) was used for this period.

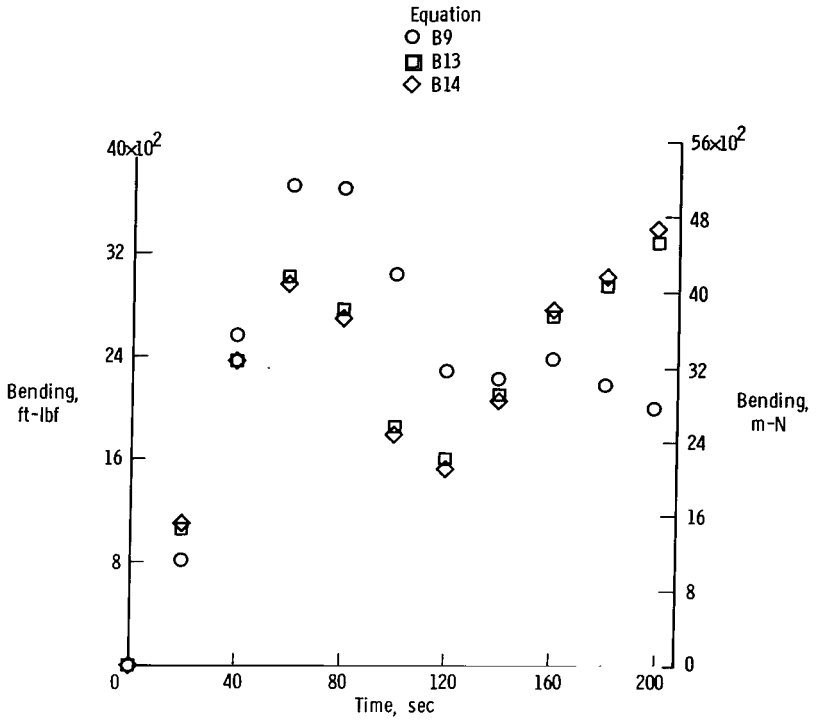

(b) Bending moment.

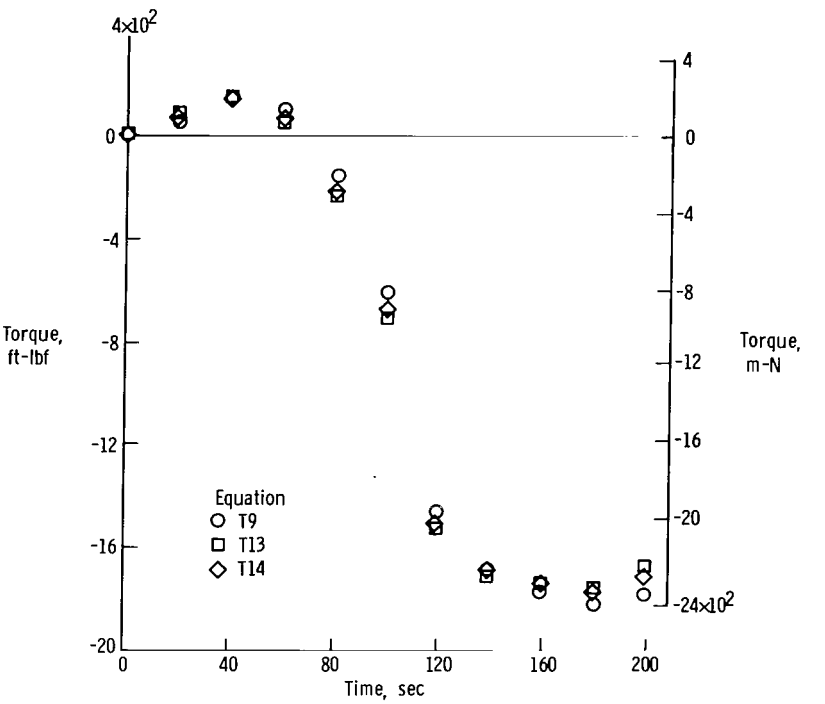

(c) Torque.

Figure 12. Concluded.

These loads are high and unpredictable and would represent such large errors compared with expected flight loads (normally less than 6000 lbf (26,700 N)) that the measurements would be invalid.

Data from flight-heating simulations are valuable not only in reducing errors such as those of figure 12 but also for selecting the strain-gage bridges to be used in the development of load equations. Such factors as the type of strain-gage bridge and its location on a structure can be optimized to provide minimum response to a severe thermal environment; however, it is extremely difficult, if not impossible, to predetermine the bridge responses with enough confidence to establish reliable equations and loads.

There is a point at which a simulation is so inadequate that it is useless. This point is reached when the error in the load measurements due to simulation inaccuracy equals the error due to neglecting the effects of the thermal environment. In an effort to establish the accuracy of loads that would be calculated by correcting flight data with the data from the standard simulation, the standard deviations for equations S9, S13, S14, B9, B13, B14, T9, T13, and T14 were calculated by using the following equations (ref. 6):

$$\sigma_s^2 = \sum_{k=1}^{m} (A_k^2 \sigma_{g_k}^2)$$

$$\sigma_b^2 = \sum_{k=1}^{m} (B_k^2 \sigma_{g_k}^2)$$

$$\sigma_t^2 = \sum_{k=1}^{m} (C_k^2 \sigma_{g_k}^2)$$

The standard deviations of the bridge outputs σ_g were assumed to be the maximum differences at each specific time between the outputs of the standard simulation and the simulation-variation tests (excluding test 1). Examples of standard deviations are shown for strain-gage bridge 2 in figure 10(a). The standard deviations for the equations are shown plotted as a function of time in figure 13. The load deviations are much smaller than the loads of figure 12, which indicates that the simulation would be a valuable tool for reducing errors in load measurements due to thermal effects. The inaccuracy of the simulation, nevertheless, still introduced much uncertainty into the results; it is believed that the number of strain-gage bridges available for consideration in the load equations influences the errors in the loads. As the number of bridges with favorable responses to the thermal environment of the simulation increases, the possibility of obtaining equations with small standard deviations due to thermal outputs increases.

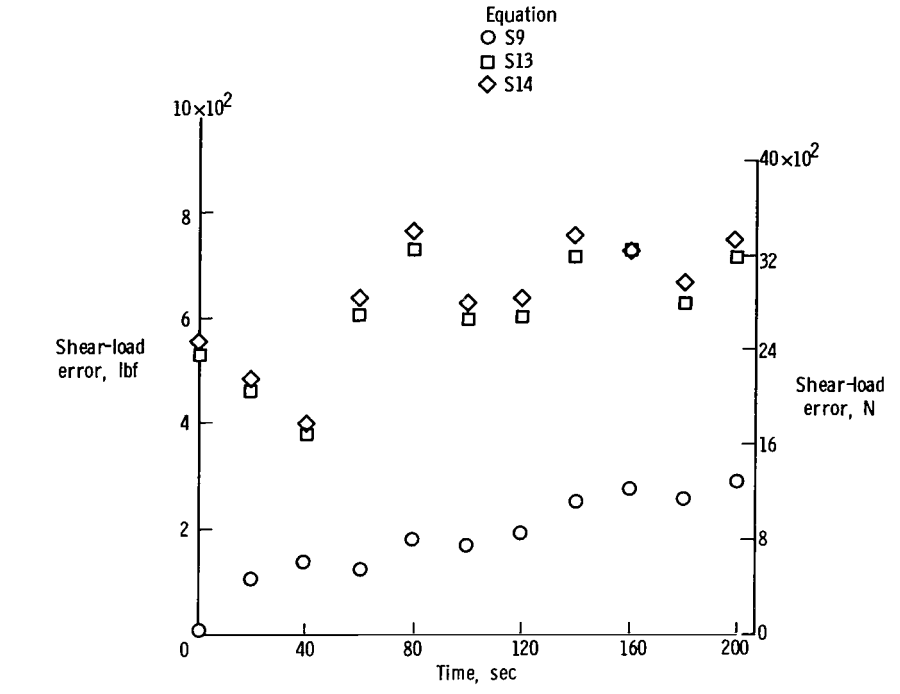

(a) Shear.

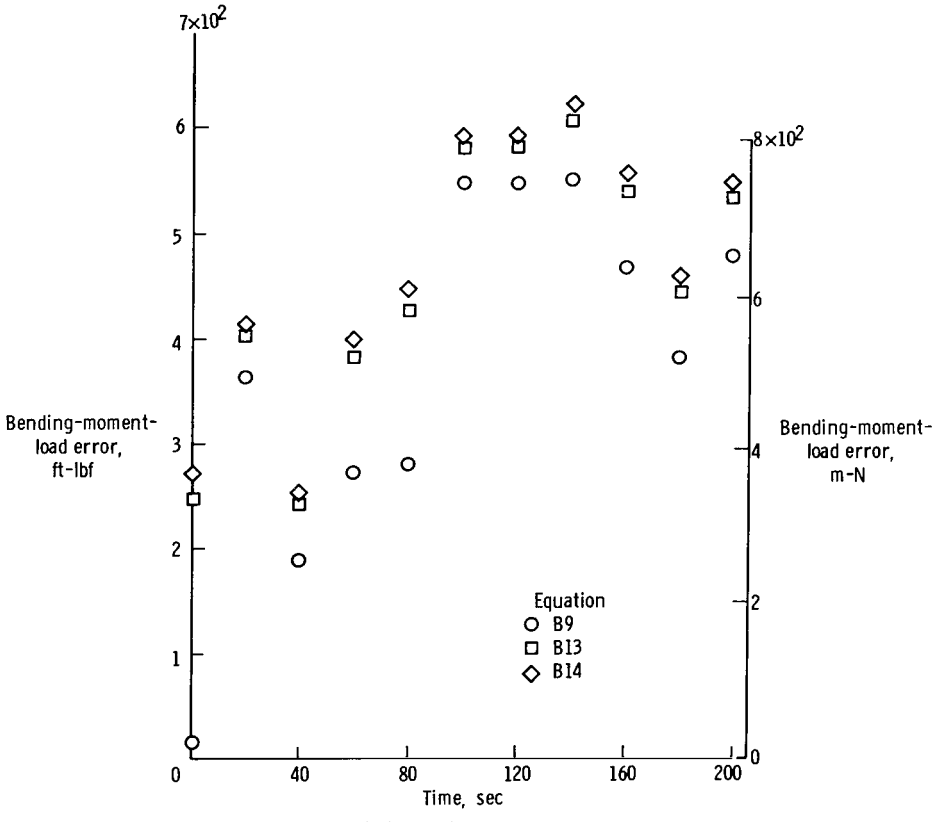

(b) Bending moment.

Figure 13. Standard-deviation time histories for loads calculated from equations and based on the simulation data.

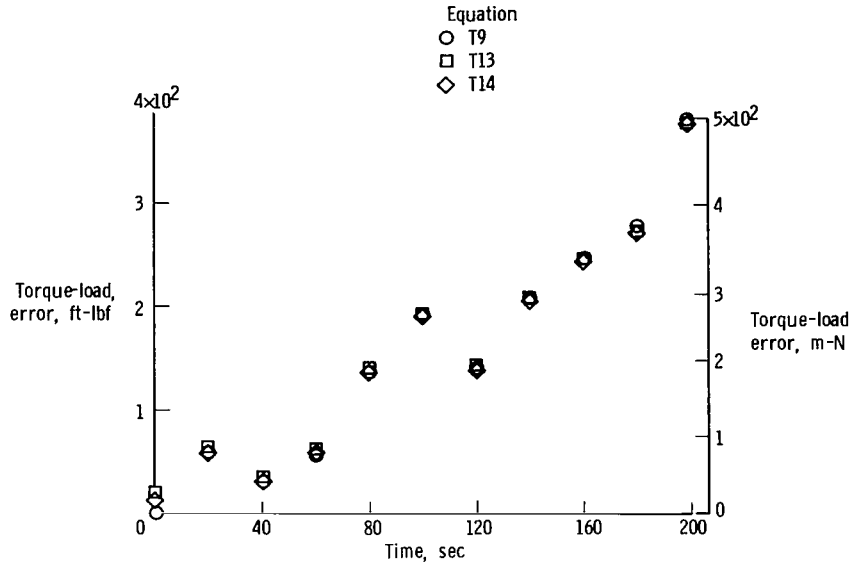

(c) Torque.

Figure 13. Concluded.

Figure 14 shows the total shear-load error due to the summation of the standard deviations at a test time of 100 seconds and the average absolute errors as a function

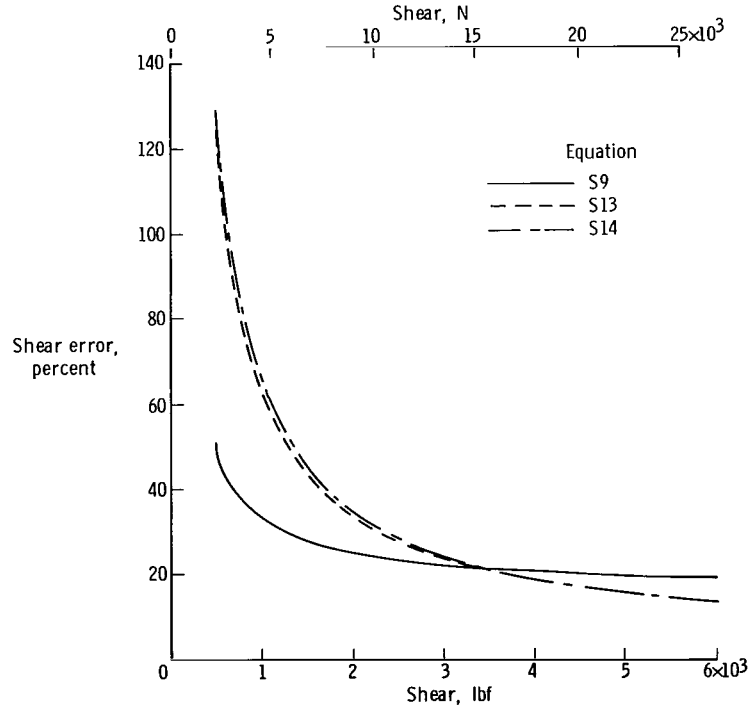

Figure 14. Total shear-load error at a test time of 100 seconds as a function of shear load.

of the shear load for three equations. It is interesting to note that below a shear load of 3400 pounds force (15,120 newtons), equation S9 has a lower error than equations S13 and S14; equation S9 also has the largest average absolute equation error. (See table III.) The magnitudes of the shear-load errors for these equations are higher than normally expected. However, the figure still illustrates that, in certain strain-gage applications in which thermal environment is a factor, it is necessary to consider more than just the equation errors when evaluating the equations that are to be used to calculate loads. An investigation such as discussed in this report may be required to make the evaluation.

Figure 14 and table III further illustrate that the slightly lower average absolute error of equation S14 as compared with that of equation S13 does not justify the use of the additional strain-gage bridge in the equation. The simulation (standard deviation) error produced by the extra bridge more than offsets the advantages of the lower error of equation S14.

CONCLUDING REMARKS

A laboratory investigation was conducted to study the feasibility of using flight-heating simulation as a means of determining the temperature effects on flight-loads measurements with strain gages. Aerodynamic-flight temperatures were simulated by utilizing liquid-nitrogen cooling and radiant heating to obtain strain-gage responses due to cooling and heating for comparison with typical strain-gage responses due to aerodynamic loads.

The thermal effects of the simulation on strain-gage responses, if ignored, were found to be significant enough to invalidate load measurements if a flight-loads program were conducted. It was determined that simulating the heating of the structure yielded repeatable thermal responses of the strain gages and that these responses may be useful in correcting data which include both the thermal and aerodynamic-load responses.

If a heating simulation and the error perturbations of the simulation are utilized in conjunction with a flight-loads program, two important factors can be determined prior to flight testing for loads measurements.

1. The ratio of the thermal output of the strain gages due to flight temperatures to the anticipated aerodynamic-load output of the strain gages.

2. The ratio of the range of strain-gage thermal outputs due to the error perturbations to the range of the anticipated strain-gage outputs due to aerodynamic loads.

If strain-gage combinations in which both of these ratios are small can be found, satisfactory loads data can be expected from flight tests supported by ground heating simulations.

When strain-gage bridges, subjected to conditions that produce thermal outputs, are used in load equations, the number of bridges should be minimized consistent with acceptable equation error. Although this may be true regardless of whether thermal

outputs are present, it is most important when thermal outputs are a factor because of added temperature-induced errors. It was shown that the improvement of equation accuracy that resulted from adding a bridge to an equation (5-bridge equation versus 4-bridge equation) did not improve the overall load accuracy even though the 5-bridge equation had the lowest average absolute error. The heating-simulation tests were also shown to be valuable as an aid in selecting the best load equations; it was shown that, below a certain load level, an equation with a higher average absolute equation error gave better results than another equation with a lower error.

Flight Research Center,
National Aeronautics and Space Administration,
Edwards, Calif., December 12, 1969.

APPENDIX

CONVERSION OF U. S. CUSTOMARY UNITS TO SI UNITS

The International System of Units (SI) was adopted by the Eleventh General Conference on Weights and Measures, Paris, October 1960, in Resolution No. 12 (ref. 3). Conversion factors for the units used herein are given in the following table:

Physical quantity	U. S. Customary Unit	Conversion factor*	SI unit
Length	ft	0.3048	m
	in.	2.54	cm
Temperature	°R = °F + 460	0.556	°K
Force	lbf	4.448	N

*Multiply value given in U. S. Customary Unit by conversion factor to obtain equivalent value in SI Unit.

REFERENCES

1. Skopinski, T. H.; Aiken, William S., Jr.; and Huston, Wilber B.: Calibration of Strain-Gage Installations in Aircraft Structures for the Measurement of Flight Loads. NACA Rep. 1178, 1954.

2. Fields, Roger A.; and Vano, Andrew: Evaluation of an Infrared Heating Simulation of a Mach 4.63 Flight on an X-15 Horizontal Stabilizer. NASA TN D-5403, 1969.

3. Mechtly, E. A.: The International System of Units - Physical Constants and Conversion Factors. NASA SP-7012, 1964.

4. Quinn, Robert D.; and Olinger, Frank V. (With appendix A by James C. Dunavant and Robert L. Stallings, Jr.): Heat-Transfer Measurements Obtained on the X-15 Airplane Including Correlations With Wind-Tunnel Results. NASA TM X-1705, 1969.

5. Sefic, Walter J.; and Anderson, Karl F.: NASA High Temperature Loads Calibration Laboratory. NASA TM X-1868, 1969.

6. Young, Hugh D.: Statistical Treatment of Experimental Data. McGraw-Hill Book Co. Inc., c. 1962.

NASA-Langley, 1970 —— 32 H-597

NATIONAL AERONAUTICS AND SPACE ADMINISTRATION
WASHINGTON, D. C. 20546

OFFICIAL BUSINESS

FIRST CLASS MAIL

POSTAGE AND FEES PAID
NATIONAL AERONAUTICS AND
SPACE ADMINISTRATION

POSTMASTER: If Undeliverable (Section 158 Postal Manual) Do Not Return

"The aeronautical and space activities of the United States shall be conducted so as to contribute . . . to the expansion of human knowledge of phenomena in the atmosphere and space. The Administration shall provide for the widest practicable and appropriate dissemination of information concerning its activities and the results thereof."

—NATIONAL AERONAUTICS AND SPACE ACT OF 1958

NASA SCIENTIFIC AND TECHNICAL PUBLICATIONS

TECHNICAL REPORTS: Scientific and technical information considered important, complete, and a lasting contribution to existing knowledge.

TECHNICAL NOTES: Information less broad in scope but nevertheless of importance as a contribution to existing knowledge.

TECHNICAL MEMORANDUMS: Information receiving limited distribution because of preliminary data, security classification, or other reasons.

CONTRACTOR REPORTS: Scientific and technical information generated under a NASA contract or grant and considered an important contribution to existing knowledge.

TECHNICAL TRANSLATIONS: Information published in a foreign language considered to merit NASA distribution in English.

SPECIAL PUBLICATIONS: Information derived from or of value to NASA activities. Publications include conference proceedings, monographs, data compilations, handbooks, sourcebooks, and special bibliographies.

TECHNOLOGY UTILIZATION PUBLICATIONS: Information on technology used by NASA that may be of particular interest in commercial and other non-aerospace applications. Publications include Tech Briefs, Technology Utilization Reports and Notes, and Technology Surveys.

Details on the availability of these publications may be obtained from:

SCIENTIFIC AND TECHNICAL INFORMATION DIVISION

NATIONAL AERONAUTICS AND SPACE ADMINISTRATION

Washington, D.C. 20546